Carbon dioxide flow and interactions in a high rank coal

Permeability evolution and reversibility of reactive processes

Hadi Mosleh, Mojgan; Turner, Matthew; Sedighi, Majid; Vardon, Philip J.

DOI
10.1016/j.ijggc.2018.01.002

Publication date
2018

Document Version
Final published version

Published in
International Journal of Greenhouse Gas Control

International Journal of Greenhouse Gas Control 70 (2018) 57–67

Contents lists available at ScienceDirect

International Journal of Greenhouse Gas Control

journal homepage: www.elsevier.com/locate/ijggc

Carbon dioxide flow and interactions in a high rank coal: Permeability evolution and reversibility of reactive processes

Mojgan Hadi Mosleh[a,b,*], Matthew Turner[a,c], Majid Sedighi[a,b], Philip J. Vardon[a,d]

[a] Geoenvironmental Research Centre, School of Engineering, Cardiff University, Newport Road, Cardiff, CF24 3AA, UK
[b] School of Mechanical, Aerospace and Civil Engineering, The University of Manchester, Manchester, M13 9PL, UK
[c] IHS Global Limited, Enterprise House, Cirencester Road, Tetbury, GL8 8RX, UK
[d] Section of Geo-Engineering, Faculty of Civil Engineering and Geosciences, Delft University of Technology, 2600 GA, Delft, The Netherlands

ARTICLE INFO

Keywords:
Carbon sequestration
Anthracite coal
Core flooding
Permeability
Matrix swelling
CO_2 adsorption
South Wales coalfield

ABSTRACT

Uncertainties exist on the efficiency of CO_2 injection and storage in deep unminable coal seems due to potential reduction in the permeability of coal that is induced by CO_2 adsorption into the coal matrix. In addition, there is a limited knowledge about the stability of CO_2 stored in coal due to changes in gas partial pressure caused by potential leakage. This paper presents an experimental study on permeability evolution in a high rank coal from South Wales coalfield due to interaction with different types of gases. The reversibility of the processes and stability of the stored CO_2 in coal are investigated *via* a series of core flooding experiments in a bespoke triaxial flooding setup. A comprehensive and new set of high-resolution data on the permeability evolution of anthracite coal is presented.

The results show a considerable reduction of permeability above 1.5 MPa CO_2 pressure that is correlated with the coal matrix swelling induced by CO_2 adsorption. Notably studied in this work, the chemically-induced strain due to gas sorption into coal, that has been isolated and quantified from the mechanically-induced strain as a result of changes in effective stress conditions. The results of post-CO_2 core flooding tests using helium (He), nitrogen (N_2) and methane (CH_4) demonstrated a degree of restoration of the initial permeability. The injection of N_2 showed no significant changes in the coal permeability and reversibility of matrix swelling. The initial permeability of the coal sample was partially restored after replacing N_2 by CH_4. Observation of permeability evolution indicates that the stored CO_2 has remained stable in coal under the conditions of the experiments.

1. Introduction

Emerging interest in deep subsurface energy applications related to geological carbon sequestration has highlighted the importance of an in-depth understanding of the complex physical and chemical phenomena that can occur during gas-rock interactions. Among those are the processes related to gas flow in coal, which are relevant to applications such as CO_2 sequestration in unminable coal seams and coalbed methane recovery. Complex and coupled physical, chemical and mechanical processes can occur during the flow of gas species in coal, affecting the key flow property of the coal, *i.e.* permeability. This is highlighted for the case of CO_2 interaction with coal due to the chemical and physical changes in the coal microstructure during adsorption and desorption (White et al., 2005).

It has been shown that the permeability of coal to gas species is dependent on several factors, including cleat and fracture systems (Harpalani and Chen, 1997; Olson et al., 2009), porosity, type of gas and pressure and mechanical stresses (Somerton et al., 1975; Palmer and Mansoori, 1998; Sasaki et al., 2004), fracture orientation (Laubach et al., 1998), and the effects of matrix swelling/shrinkage induced by gas sorption. The permeability of coal can decrease with an increase in the effective stress (*e.g.*, McKee et al., 1988; Jasinge et al., 2011). An increase in the effective stress can cause compression of the pore space available for gas flow, resulting in permeability reduction (Ranjith and Perera, 2011). It has been shown that the uptake or release of CO_2 and CH_4 is a combination of adsorption or desorption processes together with matrix swelling and shrinkage (Mazzotti et al., 2009). The amount of swelling depends on a number of parameters, including the structure and properties of the coal, gas composition, confining stress, pore pressure, temperature, fracture geometry and moisture content (Wang et al., 2013).

Compared to the extensive reported studies related to the adsorption and desorption of gases in coal (mostly on powdered samples), a limited number of experimental investigations have been reported on

* Corresponding author at: School of Mechanical, Aerospace and Civil Engineering, The University of Manchester, Manchester, M13 9PL, UK.
E-mail address: mojgan.hadimosleh@manchester.ac.uk (M. Hadi Mosleh).

https://doi.org/10.1016/j.ijggc.2018.01.002
Received 25 April 2017; Received in revised form 23 November 2017; Accepted 8 January 2018
Available online 04 February 2018
1750-5836/

gas transport and reactions in intact coal samples based on core flooding experiments. Tsotsis et al. (2004) reported core flooding experiments to study the mechanisms involved in CO_2 sequestration in a highly volatile bituminous coal. Mazumder and Wolf (2008) conducted core flooding experiments on dry and wet coal samples from the Beringen coal mines in Belgium, the Silesian coalfield in Poland, and the Tupton coalfields in the UK. Yu et al. (2008) performed gas storage and displacement experiments on coal samples originated from the Jincheng and Luan mines, Qinshui basin, North China. Wang et al. (2010) have reported core flooding experiments on high volatile bituminous coal from the Bowen Basin, Australia, and van Hemert et al. (2012) conducted a series of gas storage and recovery experiments (ECBM) on coal samples from Nottinghamshire by injecting N_2, CO_2 and mixtures of these two gases. Similarly, Connell et al. (2011) studied CH_4 displacement experiment with N_2 on a coal sample from The Bowen Basin, Australia at low and high gas injection pressures up to 10 MPa. Gas adsorption and desorption in the coal matrix has been shown to be an influential factor in permeability evolution by inducing swelling and shrinkage in coal matrix. Massarotto et al. (2007) observed permeability increases between 100 to 1200% during CH_4 desorption, compared to permeability decreases of 60–80% during CO_2 adsorption. In a study by Harpalani and Mitra (2010), the reduction of permeability to CH_4 was found to be approximately 25% of the original value, whereas the permeability to CO_2 was found to be 40% less than that to CH_4. It was reported that at elevated gas pressures, the swelling increased nearly linearly with the amount of CO_2 adsorbed (van Bergen et al., 2009). At pressures higher than 8 MPa, the gas adsorption continued to increase but the coal matrix volume remained constant, *i.e.* no coal matrix swelling occurred (Harpalani and Mitra, 2010; Kelemen et al., 2006; Gensterblum et al., 2010). Harpalani and Mitra (2010) showed that the volumetric strain of coal due to CO_2 or CH_4 adsorption followed a Langmuir-type model.

Despite extensive efforts to explore the complex and coupled phenomena involved in gas-coal interactions, understanding of the processes that can occur when CO_2 is injected into the coal and stability of the adsorbed gas in coal is incomplete. In particular, there is limited experimental knowledge related to the behaviour of high rank coals, *i.e.* anthracite, during flow and interaction with different gases. Modelling concepts have been developed in the last two decades to simulate the flow of gas in fractured rock including coal (*e.g.* Shi and Durucan, 2003; Salimzadeh and Khalili, 2015; Hosking, 2014) that are usually based on single or double porosity approaches. These models are usually based on mechanistic approaches that require appropriate constitutive relationships (*e.g.* gas permeability model) and experimental data for testing. Appropriate models/constitutive relationships for coal permeability should reflect the chemo-mechanics of the carbon sequestration and/or enhanced coalbed methane recovery problem that require experimental dataset for testing and evaluation.

The investigation presented in this paper aims to address two key phenomena related to flow of gases in a high rank coal: i) the permeability evolution of coal to different gas species under a range of gas pressures and stress conditions, with particular focus on the adsorption induced coal matrix swelling and permeability degradation during CO_2 injection, and ii) the reversibility of reactive transport processes and stability of CO_2 adsorbed in coal based on indirect observations of permeability evolution. The latter has been achieved by altering the partial gas pressure in coal *via* a sequence of core flooding experiments using different types of gases. These are important aspects related to i) the efficiency of CO_2 storage and potential changes in the storage capacity due to permeability evolution, and ii) the stability of stored CO_2 within the reservoir in case of any changes in gas partial pressure due to potential leakage events.

A novel sequence of core flooding experiments has been designed and conducted in two stages (Fig. 1). In Stage 1, permeability evolution and deformation of the coal sample by exposure to He, N_2 and CO_2 were studied for a range of gas injection pressures and confining stresses, and

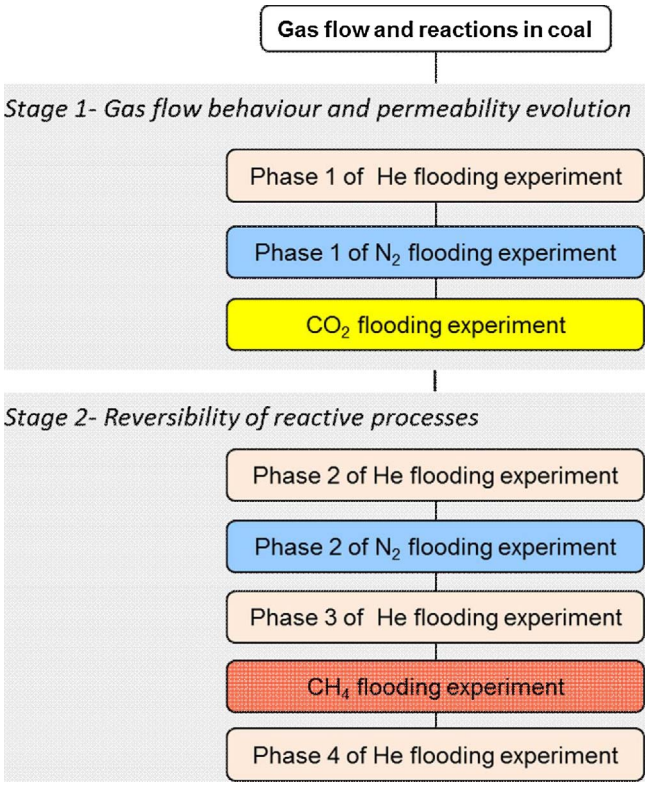

Fig. 1. The flow diagram of the experimental studies on gas flow behaviour in coal and permeability evolution.

in Stage 2, the same coal sample (after interactions with CO_2) was subjected to He, N_2, and CH_4 injections and due to the reduction of CO_2 partial pressure in the cleats, changes in intrinsic permeability was used as an indication of CO_2 desorption.

2. Materials and methods

2.1. Triaxial core flooding setup

The experimental facility developed and used consists of i) a high pressure triaxial core flooding system by which the transport and deformation properties can be measured and studied, ii) a pressure control system, iii) a temperature control system, and iv) the ancillary system including pure and mixed gas supply and analysis units (Hadi Mosleh et al., 2017b). A schematic diagram of the developed laboratory facility is presented in Fig. 2.

The triaxial cell includes a base pedestal, a top-cap, an internal submersible load cell, and local strain transducers. The core sample sits within a rubber sleeve (Fig. 3a), and the gas passes through a porous plate at the bottom of the sample. Then it leaves the cell through a similar arrangement at the top after having passed through the test core. Two axial and one radial local strain transducers (Linear Variable Differential Transformer (LVDT) from GDS Instruments) are attached to the sleeve (Fig. 3a) in order to measure the volumetric deformation of the sample under axial and radial strain conditions. In addition, a ± 0.025 m displacement transducer with an accuracy of 0.25% has been used to measure the axial displacement of the sample. A Mass Flow Meter capable of measuring high flow rates up to 17×10^{-6} m^3/s (1 L/min) was used that is capable of working under both subcritical and supercritical conditions, with pressures up to 20 MPa.

The pressure control system includes a pressure-volume controller to control the confining pressure and a high pressure regulator with a needle valve to control the gas pore pressure. Two 32 MPa in-line pore pressure transducers were selected to measure the inlet and the outlet

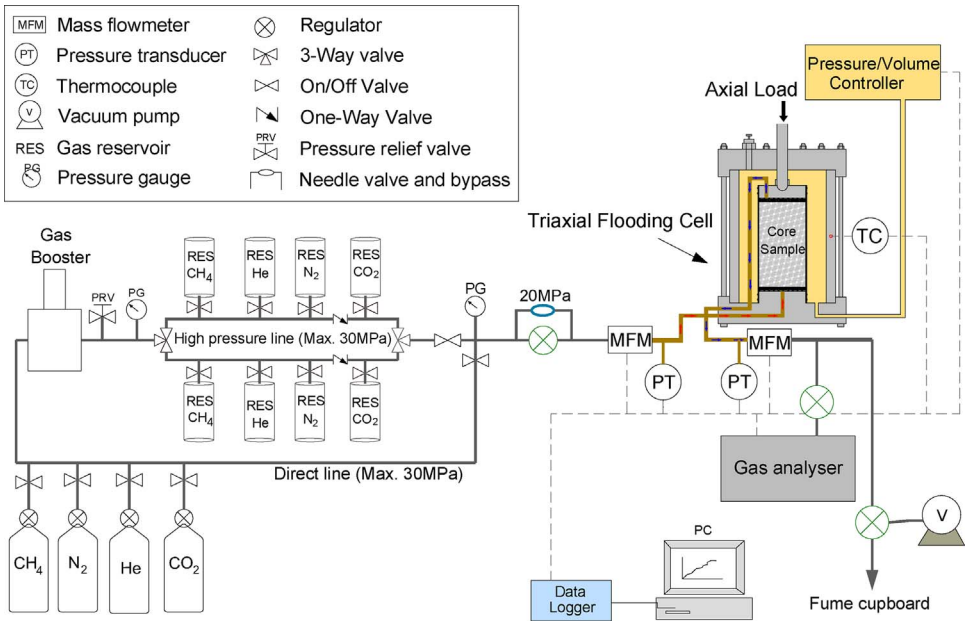

Fig. 2. A schematic diagram of the developed laboratory facility (Hadi Mosleh et al., 2017a).

gas pressures. The confining system consists of a 32 MPa pressure/volume controller with a $2 \times 10^{-4}\,m^3$ oil reservoir. Volume changes can be measured and displayed to $1 \times 10^{-9}\,m^3$ (0.001cc). In order to provide the confining pressure around the sample, silicone oil 350 (Polydimethylsiloxane), as recommended by ASTM STP-977 (ASTM Standards, 1988) has been used.

In order to control the temperature of the testing sample and providing isothermal conditions, a climate control system was installed. The system comprises four heating elements (Fig. 3b) and a programmable controller. Heating elements provide constant temperature around the sample from ambient temperature, to up to 338 K (65 °C). Temperature within the sample is measured using three thermocouples attached to the top, middle and bottom of the sample.

The ancillary system comprises two main sections, including the gas

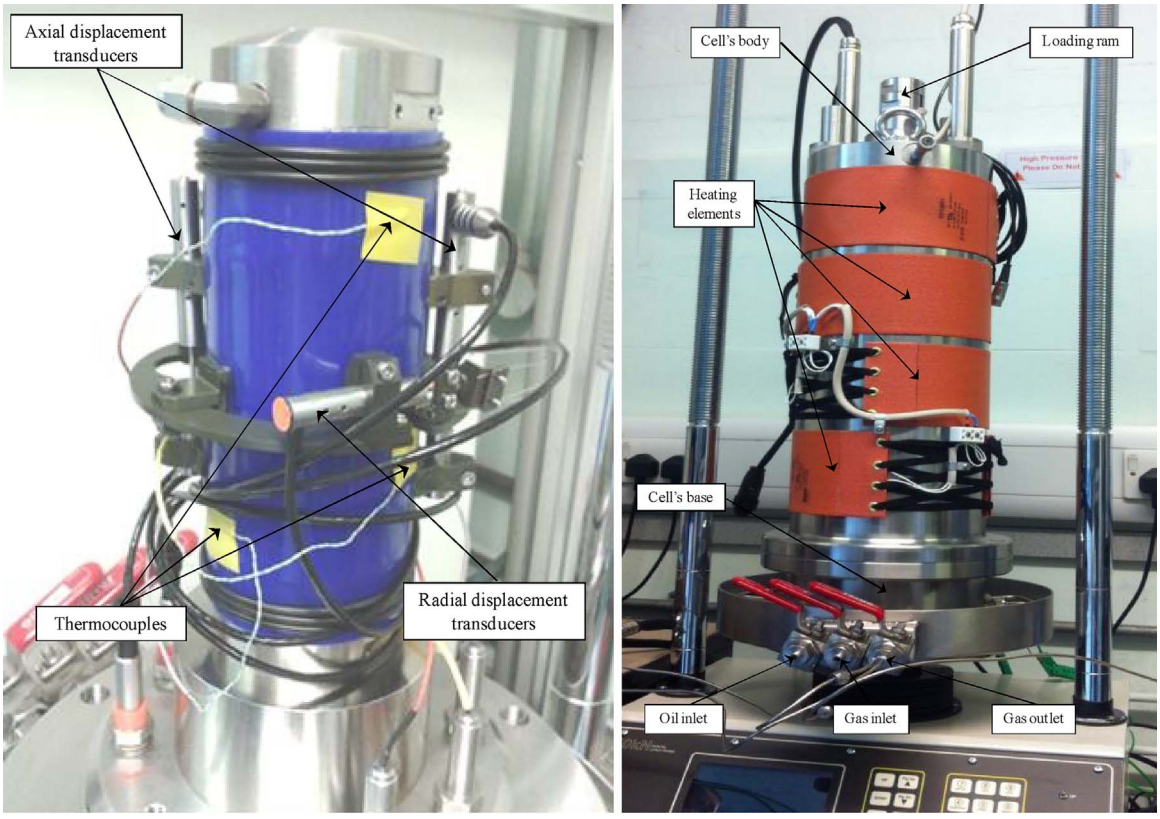

(a) (b)

Fig. 3. Triaxial core flooding cell developed and used: (a) Displacement transducers and thermocouples attached to the sample, and (b) The top cap with the heating elements, mounted on the load frame (Hadi Mosleh, 2014).

supply unit and gas analysing unit. The gas supply system was designed to deliver different gases with controlled pressure and temperature to the triaxial core flooding system at pressures up to 30 MPa and temperatures up to 338 K (65 °C). A Haskel air driven gas booster (model AG-62-50341) has been used to pressurise the gas and a set of gas reservoirs have been used to store the pressurised gases to be used for high gas demand experiments. A vacuum pump was employed to evacuate the entire system including the dead volumes inside the pipes and the valves to avoid any contamination of injecting gases with the residual gases from previous tests. The composition of the outflow gases can be determined using an Emerson X-Stream general purpose gas analyser (standard 19″/3HU version). More details related to the design and development of the experimental setup can be found in Hadi Mosleh et al. (2017b).

2.2. Preparation and properties of the coal sample

The coal sample used in the present study was obtained from the Six Foot seam (Carboniferous) of the Unity coal mine in South Wales, UK. A series of coal characterisation analyses have been conducted to determine key parameters including moisture content, ash content, and volatile matter as well as elemental compositions including sulphur content and carbon content. Table 1 presents a summary of the physical and chemical properties of the coal sample.

Large blocks of coal were collected from the 6-ft seam located at approximate depth of 550 m. The 70 mm-diameter core samples were drilled out from the coal blocks using a coring machine and were then cut into the required lengths using a diamond saw. In order to allow a uniform distribution of the axial stresses to both ends of the sample and to prevent breakage of the coal samples under high stress conditions, the ends of the specimens were ground and made parallel to each other using a fine sand paper. The core samples were then air-dried for 24 h and wrapped in a plastic cling film. The samples were stored in a refrigerator to be used for the tests.

2.3. Experimental procedure and measurement method

A core sample with 7 mm diameter and 120 mm length was carefully wrapped with a thick PTFE (Polytetrafluoroethylene) tape before placing in a silicon rubber sleeve. The PTFE tape was used as a non-reactive material which prevents gas diffusion through the rubber membrane into the silicone oil as well as protecting the membrane from any sharp edges that may remain on the coal surface. A 1.5 mm thick blue silicone rubber has been used as the membrane (Fig. 3a). The displacement transducers, two axial and one radial, and the thermocouples were then attached to the sample (Fig. 3a). Top cap was placed on the base pedestal and the cell was filled with the silicone oil (Fig. 3b). The temperature of the system was set to the desired value and kept constant throughout the test. It is noted that under the *in situ* conditions, zero-strain or uniaxial strain conditions are expected, however, most of the experimental investigations related to the coal permeability variations with effective stress have been conducted under the non-zero strain conditions (Harpalani and Mitra, 2010), *i.e.* the coal samples have been allowed to expand in both axial and radial directions. Attempts were made by Harpalani and Mitra (2010) to maintain zero-strain conditions during a CO_2 core flooding experiment, however the excess stress required maintaining this condition was very large, resulting in sample failure.

Table 1
Physical and chemical properties of the coal sample.

Moisture (%)	1.19	Carbon (%)	86.42
Sample diameter (mm)	7	Volatile matter (%)	9.56
Sample length (mm)	120	Fixed carbon (%)	84.39
Bulk density (kg/m^3)	1495	Sulphur (%)	0.79
Porosity (−)	0.05	Ash (%)	4.85

A confining pressure of 1 MPa was applied, and the sample was subjected to a vacuum for 24 h. After the vacuum process, the downstream valve was closed and the experimental gas was injected at the upstream end. The upstream pressure was increased step by step to the desired level. Gas injection at fixed pressure was continued to saturate the sample with gas. Depending on the test conditions and gas type, saturation was achieved within 3–6 days. The condition for achieving the saturation state was based on a pressure decrease less than 0.05 MPa over a 24 h period as suggested by van Hemert et al. (2012).

The steady-state method was then used to estimate the permeability of the coal samples. The confining pressure was maintained at the desired pressure and increased step by step. The gas pressure at the upstream end was fixed, at a range of pressures. The downstream pressure was constantly kept at atmospheric pressure (0.1 MPa). Once the steady-state flow rate was achieved, the differential gas pressures and gas flow rates were recorded and permeability of the coal sample was calculated using Darcy's equation for gases (Carman, 1956):

$$k_g = \frac{2Q_0\mu_g LP_0}{A(P_{up}^2 - P_{down}^2)} \quad (1)$$

where, k_g is the gas permeability coefficient (m^2), Q_0 is the volumetric rate of flow at reference pressure (m^3/s), μ_g is the gas viscosity (Pa s), L is the sample length (m), P_0 is the reference pressure (Pa), A is the cross-sectional area of the sample (m^2), P_{up} is the upstream gas pressure (Pa), and P_{down} is the downstream gas pressure (Pa). The viscosity of gases (μ_g) was calculated based on the Sutherland formula as function of temperature (Smits and Dussauge, 2006). The results of the core flooding experiments are presented and discussed in the following sections.

3. Stage 1—gas flow behaviour and permeability evolution in coal

For the first stage, permeability evolution and deformation of the coal sample in response to the injection of He, N_2 and CO_2 were estimated at a range of gas pressures up to 5.5 MPa and confining stresses up to 6 MPa.

3.1. Helium flooding experiment

Fig. 4a presents the results of the helium flow rates *versus* differential gas pressures obtained for a range of gas injection pressures up to 5.5 MPa and confining pressures up to 6 MPa at 298 K. The results show that despite a certain pressure gradient across the sample, no apparent flow was observed and recorded at low pressures within the timescale allowed, *i.e.* 15–30 min. This effect was attributed to "threshold phenomenon" (Chen et al., 2006). Accordingly a certain nonzero pressure gradient (1.7 MPa/m) was required to initiate the flow.

The overall gas flow rate was found to increase with the increase in gas injection pressure. A maximum value of 88×10^{-6} m^3/s at approximately 5.5 MPa differential gas pressure and 6 MPa confining pressure was recorded. In addition, under constant gas injection pressures, a considerable decrease in the gas flow rate was observed as a result of increases in the confining pressure applied.

Fig. 4b presents the absolute permeability of the coal sample at different gas pressures and confining pressures. At constant confining pressure of 1 MPa, the absolute permeability of the coal sample increased considerably due to the increase in gas injection pressure and reached a maximum value of 1.35×10^{-15} m^2 (at a differential gas pressure of 0.6 MPa). The gas injection pressure was then kept constant and the confining pressure was increased to 2 MPa. As a result, permeability decreased by 68%. At constant gas injection pressures, an average permeability reduction of 54% was observed for every 1 MPa increase in confining pressure.

For low permeability coals, the flow behaviour is highly dependent

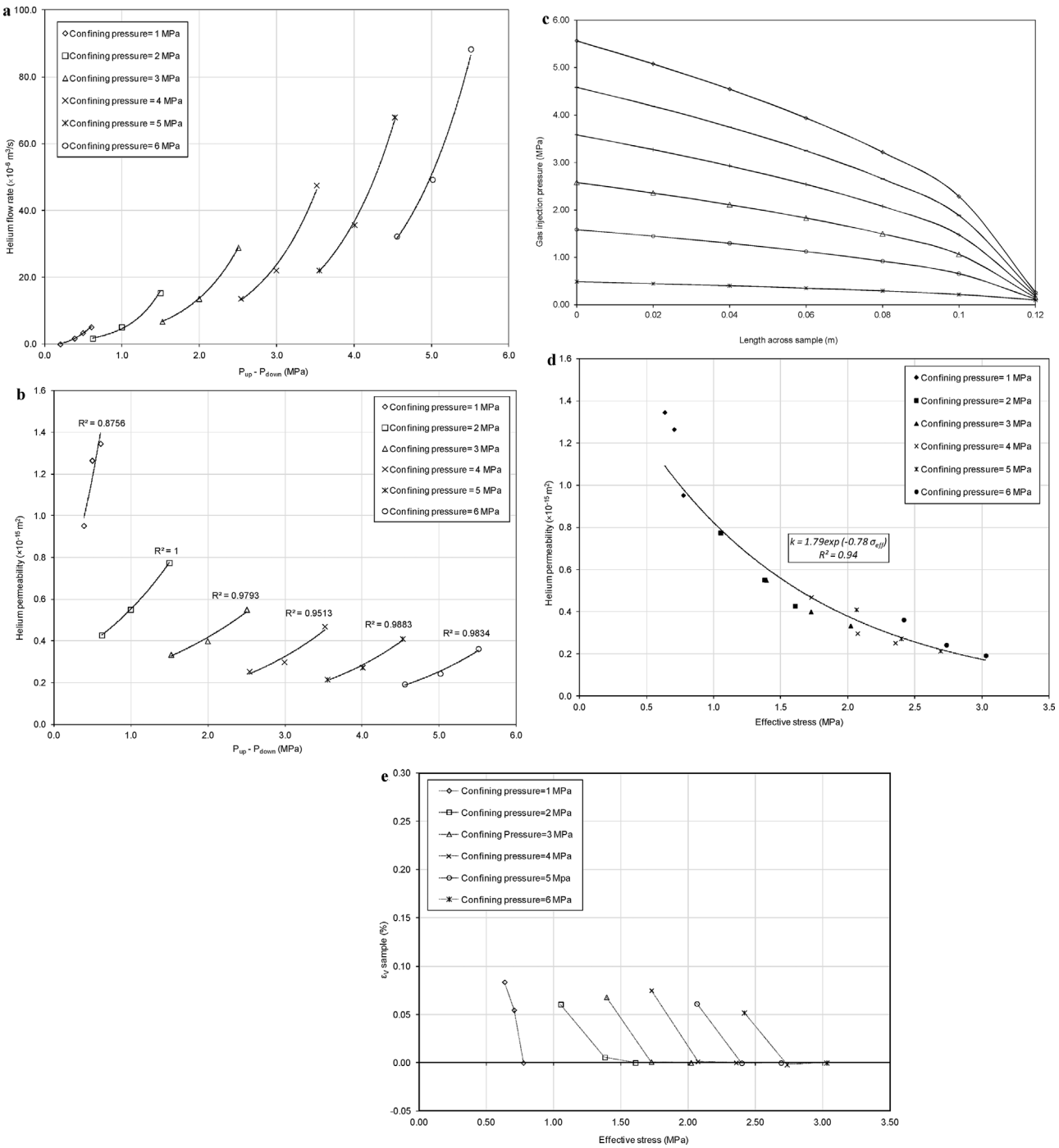

Fig. 4. (a) Variations of helium flow rates *versus* differential gas pressure between the upstream and downstream at various confining pressures (T = 298 K). (b) Variations of absolute permeability of the coal sample to helium *versus* differential gas pressure between upstream and downstream at various confining pressures (T = 298 K). (c) Variation of gas pore pressure across sample length. (d) The relationship between coal permeability to helium and effective stress (T = 298 K). (e) Variations of the volumetric expansion of the coal sample *versus* effective stress due to the increase in helium pressure at constant confining pressures (T = 298 K).

on the effective stress (Huy et al., 2010), and the effect of effective stress can be considerable in coal permeability changes. The average effective stress of coal subjected to a gas pressure can be expressed as (Harpalani and Chen, 1997):

$$\sigma_{eff} = P_c - \frac{P_{up} + P_{down}}{2} \tag{2}$$

where, σ_{eff} is the effective stress and P_c is the confining pressure.

Unlike water, gas is a compressible fluid and therefore its bulk density varies significantly. As the result, variation of gas pore pressure across sample length is not expected to be linear (Hadi Mosleh et al., 2017a). In this study, the analytical solution presented by Wu et al. (1998) has been used to estimate the changes in gas pore pressure across the sample at steady-state flow conditions:

$$P(x) = -b + \sqrt{b^2 + P_L^2 + 2bP_L + 2q_m\mu(L - x)/k_\infty\beta} \tag{3}$$

where, $P(x)$ is the gas pressure (Pa) at linear distance x(m), b is the Klinkenberg coefficient, P_L is the gas pressure at outlet boundaries of linear flow systems (Pa), q_m is the gas mass injection or pumping flux (kg/s m^2), L is the length of linear flow systems or thickness of unsaturated zone (m), k_∞ is the absolute permeability (m^2), and β is the

compressibility factor; μ viscosity (Pa s).

In order to accurately estimate variation of gas pore pressure across the sample, the length of the sample was divided into 7 sections of 0.02 m long, and for each section the average pore pressure was estimated using Eq. (3). Fig. 4c shows estimated gas pore pressure variations across sample length, using Eq. (3), for a number of gas injection pressures. The effective stress was then calculated as the difference between confining pressure and the average gas pore pressure, at each injection pressure step.

By plotting the experimental results of the coal permeability to helium *versus* effective stress, a general trend of the coal permeability reduction can be observed as a result of an increase in the effective stress (Fig. 4d). An empirical relation between the coal permeability to helium and effective stress was developed as it has been shown in Fig. 4d. The exponential function demonstrates a relatively good fit with the experimental data. The exponential relationship between the coal permeability and effective stress has been also reported by other researchers (Jasinge et al., 2011; Chen et al., 2006; Vishal et al., 2013; McKee et al., 1988, Seidle and Huitt, 1995).

The permeability of coal to helium decreased sharply at lower stress conditions. This can be attributed to the immediate closure of existing microfractures under low stress (Somerton et al., 1975; Durucan and Edwards, 1986). Therefore, only the second section of the curve can represent the deformation effects of the coal matrix under stress (Durucan and Edwards, 1986).

The variations of coal permeability with effective stress can be controlled by the compression of the pores and fracture system at high effective stresses (Somerton et al., 1975; Durucan and Edwards, 1986), or as a result of both compression and microfracturing of the coal material (Durucan and Edwards, 1986). The compressibility of the fracture system can change as the effective stress increases (Pan et al., 2010). Therefore at higher stress conditions, the effect of effective stress on coal permeability becomes less considerable. This is compatible with the observations presented in Fig. 4d.

Fig. 4e presents the results of the volumetric expansion of the coal sample due to the increase in gas pressure under constant confining pressures. At a constant confining pressure, the increase in pore pressure resulted in the decrease of the effective stress and consequently expansion of the coal sample. Overall, every 0.5 MPa increase in the mean gas pressure has induced an expansion of approximately 0.07% in the coal sample volume (under constant confining pressures). The total expansion of the coal sample due to 2.7 MPa increase in the mean gas pore pressure was estimated to be approximately 0.4%. Since helium is a non-reactive/non-adsorptive gas species, the volumetric strains of the coal sample observed are purely attributed to the mechanical deformations of the coal sample due to variations in effective stress, *i.e.* expansion and compression in response to the internal and external forces.

3.2. N_2 flooding experiment

A similar experimental procedure that was performed for the helium flow measurements was repeated for the N_2 flooding experiment and the permeability coefficients of the coal sample to N_2 were calculated using Eq. (1). The variations of N_2 permeability coefficients with differential gas pressures up to 5.5 MPa at several confining pressures are presented in Fig. 5a. At constant gas injection pressures, an average permeability reduction of 65% was observed as a result of every 1 MPa increment of confining pressure.

Fig. 5b presents the variations of coal permeability to N_2 with effective stress. Similar to the helium flooding results, overall permeability of the coal sample decreased with the increase in the effective stress. As shown in Fig. 5b, the exponential regression between the coal permeability to N_2 and effective stress is relatively poor, compared to the results of first helium flooding experiments, which may limit the application of the established exponential relationship.

The relative permeability values of the coal sample (k_r), *i.e.* $K_{(N2)}/K_{(He)}$, were also estimated based on the results of the N_2 permeability and the absolute permeability coefficients, *i.e.* He permeability, for a range of gas pressures and confining pressures and presented in Fig. 5c. In general, the relative permeability of the coal sample to N_2 was found to be much smaller than those for helium at lower pressures which can be related to the immediate closure of microfractures (Somerton et al., 1975; Durucan and Edwards, 1986) and larger kinetic diameter of N_2, *i.e.* 0.36 nm (Gan et al., 1972). Due to the small kinetic diameter, *i.e.* 0.26 nm (Mehio et al., 2014), helium can penetrate most of the pores that might not be accessible for N_2 molecules.

The hysteresis as a result of repeated loading and unloading cycles might have also led to the lower permeability of the coal sample to N_2 (Somerton et al., 1975; Dabbous et al., 1974). Dabbous et al. (1974) reported strong hysteresis due to different cleat compressibility at loading and unloading cycles. Although changes in fracture system and cleat aperture has been shown to be largely reversible at lower stress conditions (Wang et al., 2013), higher effective stresses can result in non-reversible changes such as creating new fractures or microfractures. The relative permeability of the coal sample to N_2, however, increased with an increase in gas pressure and confining pressure and reached a maximum of 70% of the helium permeability at the corresponding stress condition.

The comparative and noncumulative volumetric expansions of the coal sample due to increases in N_2 pressure at constant confining pressures are presented in Fig. 5d. In order to compare the effect of N_2 on the volumetric strains of the coal sample with the behaviour observed during helium injection, the volumetric strains from the helium flooding experiment are also included (dashed lines). The results show that the amounts of coal expansion due to N_2 injection into the coal are slightly higher than those obtained in the case of helium injection, especially at lower effective stress values.

As the effective stress increases, the expansion rate decreases that match with the results of the He flooding experiment. At constant confining pressures, an average expansion rate of 0.08% was observed as a result of 0.5 MPa increase in the gas pressure. Since the volumetric effect of N_2 on the coal matrix due to its sorption has been found to be negligible (Hadi Mosleh, 2014), it can be assumed that the volumetric deformations observed are mostly related to the mechanical deformation of the coal sample.

The results of the volumetric strains show that at higher effective stresses, the mechanical strains of the coal sample during N_2 flooding experiments are similar to those observed in the helium flooding experiments. At lower effective stresses however, the differences in volumetric deformations may be related to properties of the gas species (kinetic diameter) and the hysteresis and changes in the coal structure as a result of loading and unloading applied during previous stages of the test. Although it should be mentioned that due to complex nature of coal material, it is difficult to distinguish and isolate the magnitude of the effects of different factors on the gas flow and deformation behaviour observed for the coal sample. For instance, parameters such as the cleat compressibility which is often considered as a constant value in a certain coal might also change with changes in effective stress (Pan et al., 2010).

3.3. CO_2 flooding experiment

After the N_2 flooding experiment, the CO_2 flooding experiment was performed on the same coal sample after applying vacuum and saturating it with CO_2 at 5 MPa gas pressure for the duration of approximately 6 days. The results of permeability of the sample to CO_2 *versus* differential gas pressures at different confining pressures are presented in Fig. 6a. At constant gas pressures, every 1 MPa increase in the confining pressure resulted in an average permeability reduction of approximately 70%. More importantly, as the injection continued, the interaction between CO_2 and coal resulted in extensive coal swelling

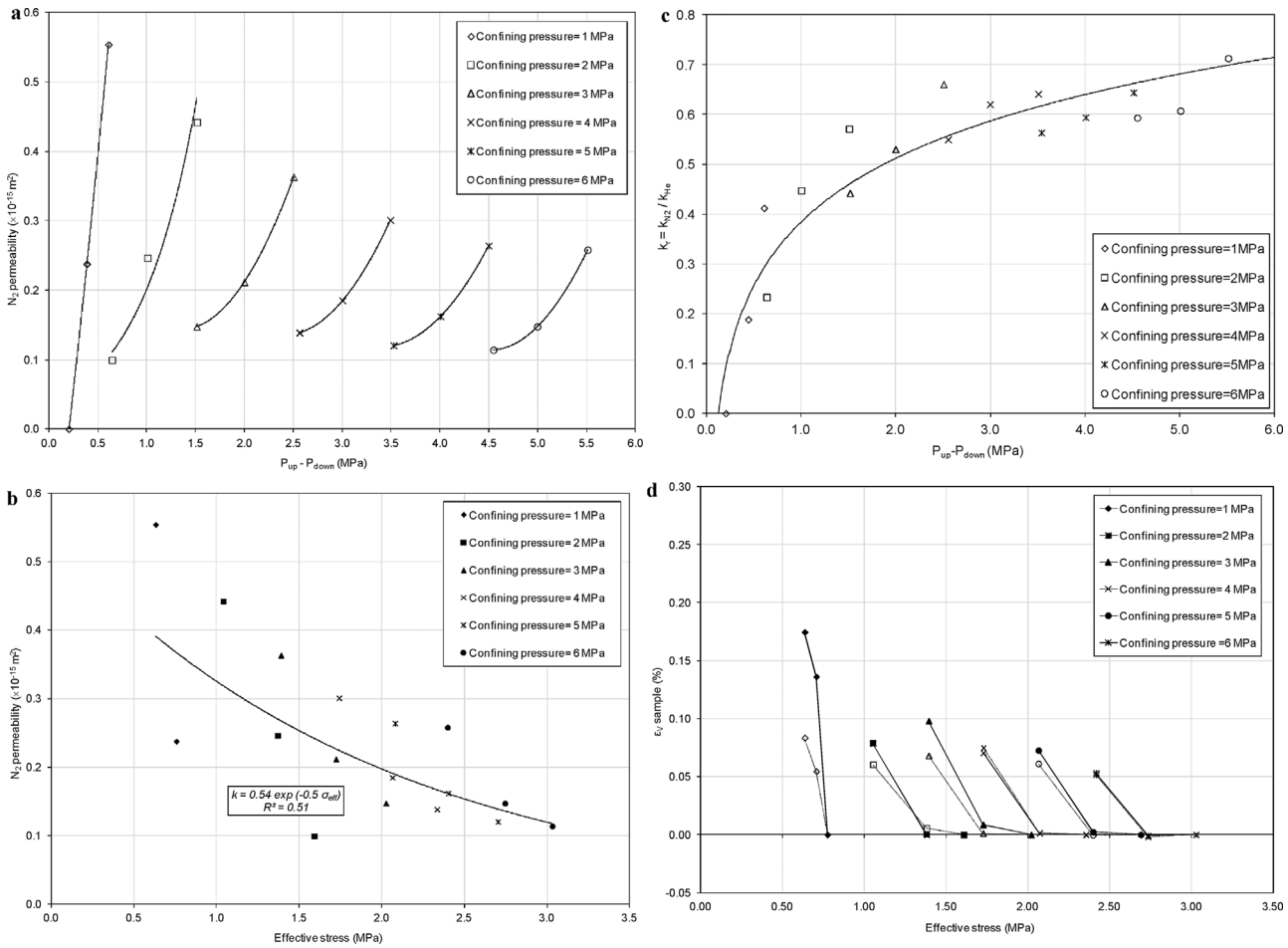

Fig. 5. (a) Variations of permeability of the coal sample to N_2 *versus* differential gas pressure at various confining pressures (T = 298 K). (b) The relationship between permeability of coal to N_2 and effective stress (T = 298 K). (c) Variations of the relative permeability (k_r) of the coal sample to N_2 with differential gas pressure at various confining pressures (T = 298 K). (d) Variations of volumetric expansion of the coal sample *versus* effective stress variations due to increase in N_2 pressure at constant confining pressures (T = 298 K); (dashed lines show the volumetric expansions of the coal sample during phase 1 of helium flooding experiment).

and consequently a reduction of gas flow and permeability of the coal sample. At confining pressure of 6 MPa, despite a 0.5 MPa of increase in the gas pressure applied the coal permeability remained almost constant. The lowest permeability value of 0.01×10^{-15} m^2 was obtained at this stage.

Permeability decline despite the increase in pore pressure at constant confining pressures has been attributed to the adsorption-induced coal swelling (Pan et al., 2010). Vishal et al. (2013) measured the permeability to CO_2 of a coal sample at 5 MPa confining pressure and gas injection pressures up to 3 MPa. It has been reported that the permeability of the coal reduced considerably with increase in injection pressure (Vishal et al., 2013). According to Wang et al. (2013), the overall change in the coal permeability is a function of the mechanical response, swelling or shrinkage of the matrix and the damage or fracture induced by the applied stress. The expansion of the coal matrix due to CO_2 adsorption leads to the closure of the cleats and fractures, which in turn reduces the permeability of coal (Siriwardane et al., 2009).

Fig. 6b presents the results of the coal permeability measurements *versus* effective stress. The coal permeability to CO_2 decreased much faster at lower stress conditions which again can be attributed to the closure of microfractures at low stresses due to the effect of CO_2 adsorbed-phase volume (Somerton et al., 1975; Durucan and Edwards, 1986) combined with the matrix swelling effect induced by CO_2 adsorption. As the experiment continued and gas pressure and confining pressure increased, the effect of the effective stress on coal permeability became less significant (Fig. 6b). The matrix swelling is likely to be the dominant factor in changes of the coal permeability. In general, the exponential relationship between the coal permeability to CO_2 and effective stress is found to be much stronger than those observed for He and N_2 (higher coefficient of determination for the case of CO_2).

The relative permeability of the coal sample to CO_2, *i.e.* $K_{(CO2)}/K_{(He)}$, is presented in Fig. 6c. As the results show, the relative permeability of the coal sample to CO_2 at its highest was less than 30% of its absolute permeability (helium permeability at corresponding pressures). Similar to the N_2 flooding experiment, this can be partly attributed to the larger kinetic diameter of CO_2 compared with helium as well as the hysteresis due to loading and unloading cycles. However, the effect of adsorbed-phase volume on microfractures might have influenced the coal permeability even before the CO_2 flow measurements, *i.e.* during saturation stage. This may explain such lower permeability of the coal sample to CO_2.

The sharp decrease in the relative permeability of coal to CO_2 at higher effective stresses is related to the effect of coal matrix swelling on cleats and fracture system at higher pressures (Jasinge et al., 2011; Vishal et al., 2013; De Silva and Ranjith, 2012). The lowest relative permeability can be observed at effective stress of 5.5 MPa (Fig. 6c) which was found to be 5% of its initial absolute permeability at corresponding stress conditions.

Similar behaviour for CO_2 permeability reduction with effective stress has been reported by other researchers. Huy et al. (2010) conducted CO_2 core flooding experiments on different coals from China, Australia, and Vietnam, to investigate the effect of effective stress on gas permeability. For their experiments, the confining stress on the coal sample was increased from 1 to 6 MPa, and the average gas pore

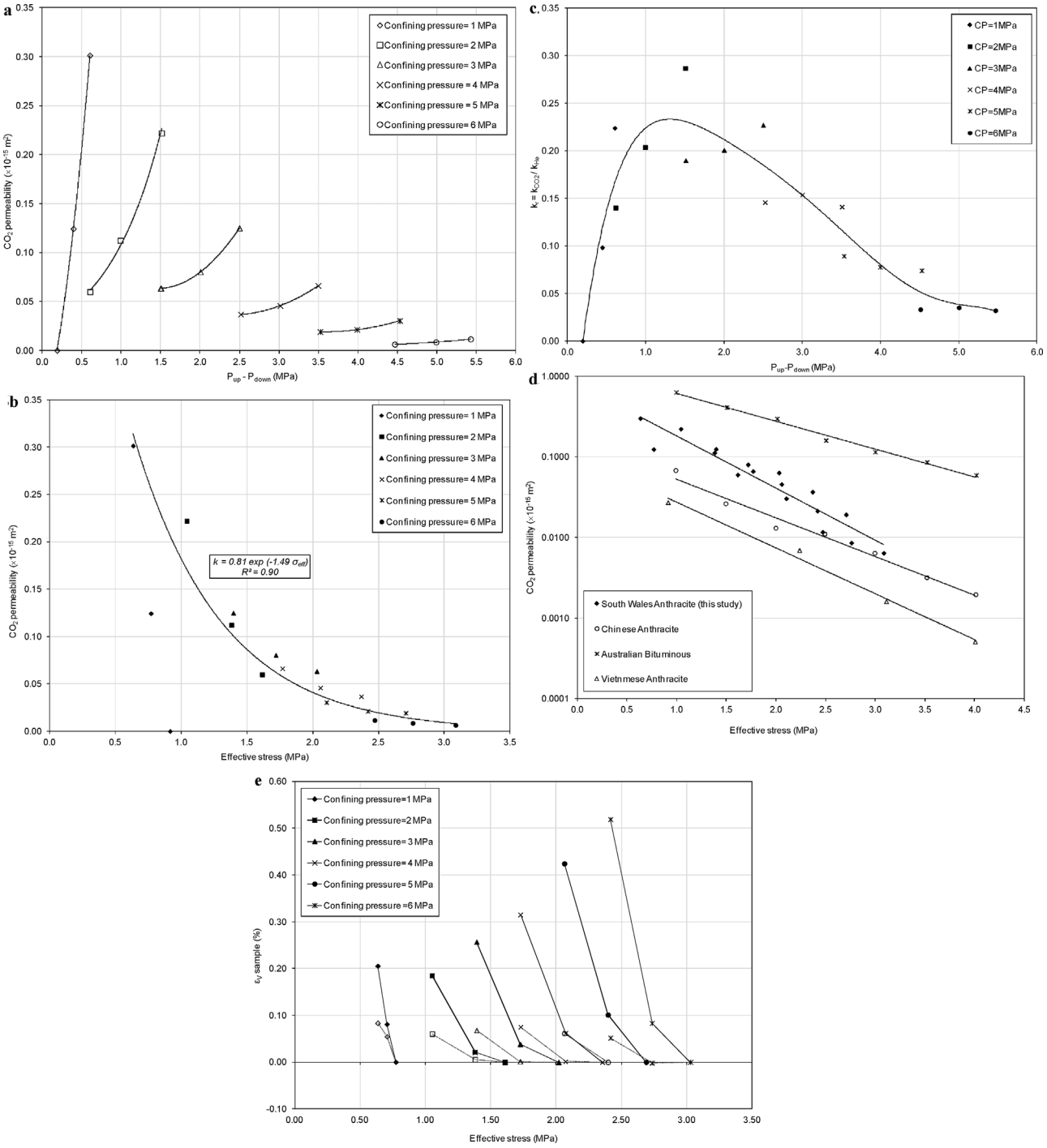

Fig. 6. (a) Variations of permeability of the coal sample to CO_2 *versus* differential gas pressure at various confining pressures (T = 298 K). (b) The relationship between permeability of coal to CO_2 and effective stress (T = 298 K). (c) Variations of the relative permeability (k_r) of the coal sample to CO_2 with differential gas pressure at various confining pressures (T = 298 K). (d) CO_2 permeability evolution with effective stress for the coal sample of this study (South Wales Anthracite) and other types of coal studied by Huy et al. (2010). (e) Variations of the volumetric expansion of the coal sample with effective stress variations due to increase in CO_2 pressure at constant confining pressures (T = 298 K); (dashed lines show the volumetric expansions of the coal sample during phase 1 of helium flooding experiment).

pressure applied was between 0.1 and 0.7 MPa. Fig. 6d shows the results of CO_2 permeability evolution with effective stress for the coal sample of this study (South Wales Anthracite) and those studied by Huy et al. (2010). From this comparison it can be postulated that the overall gas permeability behaviour of South Wales Anthracite as the result of changes in effective stress is similar to those observed and reported for other types of coal. The slight differences however can be attributed to various methods that might have been used to estimate the average pore pressure and the effective stress values (*i.e.* Eqs. (2) and (3)).

The volumetric deformations of the coal sample due to CO_2 injection at different confining pressures are presented in Fig. 6e (Dashed lines represent the results of the phase 1 of helium flooding experiment). The overall volumetric expansion of the coal sample during CO_2 flooding experiment was much higher than those for other gases. For He and N_2 flooding experiments, it was observed that although the coal sample expanded due to the increase in the pore gas pressure, the amounts of the volumetric expansion at different confining pressures were almost comparable. In the case of CO_2, however, this similarity is

not observed and the amount of coal expansion increases more clearly which can be related to the swelling effect of CO_2 adsorption on coal.

As higher injection pressure was applied, the difference between the volumetric strains observed in the He and CO_2 flooding experiments increased considerably. At the final step of the injection, the increase in the coal volume was found to be ten times more than those observed in the He flooding experiment. In general, the trend of the coal permeability variation with pore pressure was found to be opposite to that of the volumetric increase in coal. This behaviour can be attributed to the fact that coal adsorbs more CO_2 at higher injection pressures, which leads to further swelling of the coal matrix.

The coal sample exhibited 1.9% volume increase during the CO_2 flooding experiment. The swelling effect was then quantified by subtracting the mechanical effects obtained from the phase 1 of the helium flooding experiment. According to the results, the swelling effect of CO_2 in the volumetric expansion of the coal is 1.5%. It should also be mentioned that the volumetric strain measured here may have been underestimated for the matrix swelling because the cleat porosity may take part of the displacements (Vishal et al., 2013). In addition, due to the relatively short exposure of the coal sample to CO_2, the adsorption process might have not been completed and more swelling could be expected for a longer exposure.

4. Stage 2—reversibility of reactive processes

For the second stage, a sequence of He, N_2, and CH_4 injections was conducted on the same coal sample, and the reversibility of the CO_2 sorption-induced coal swelling and permeability changes investigated.

4.1. Helium flooding experiment

In this experiment, He was re-injected into the sample to study the potential changes in the intrinsic permeability and potential reversibility of the swelling process by reducing the partial pressure of CO_2 in the cleat. The experimental conditions and injection pressures were similar to those performed for the previous tests in Stage 1. The results of the coal permeability to helium obtained from the phase 2 of the helium flooding experiment are presented in Fig. 7a. For comparison, the results of the phase 1 of helium flooding experiment (before CO_2 injection) are also included in the graph (dashed lines).

The results show that the coal permeability has decreased considerably as a result of coal interactions with CO_2. The overall trend of the coal permeability remained almost steady throughout the test in comparison to the earlier tests and did not show any significant changes with the effective stress.

An overall permeability reduction of 89% was observed at lower pressures. The results of relative permeability of CO_2 to He (Fig. 6c) suggests a larger permeability reduction (nearly 95%), therefore it can be concluded that some of the coal permeability was restored due to CO_2 desorption during vacuum process and helium saturation phase. At the higher gas injection pressures and confining pressures, the coal permeability increased slightly and reached to a value of approximately $0.07 \times 10^{-15}\,m^2$, *i.e.* 75% of the initial value. The average permeability value of the coal sample was increased by 14% during the phase 2 of helium injection.

4.2. N_2 flooding experiment

Since helium is a non-adsorptive gas, its chemical interaction with coal is very limited. Although, due to an increase of helium partial pressure, CO_2 molecules can desorb first from weakly adsorbed sites, it cannot replace the strongly adsorbed CO_2 molecules in coal matrix pores (micropores). With N_2, however, the behaviour can be different. N_2 can be partially adsorbed to the coal and its replacement with some of the adsorbed CO_2 might affect the coal swelling and permeability. In order to further investigate that effect, the coal sample was subjected to the phase 2 of N_2 injections. Subsequently and in order to evaluate the effect of the phase 2 of N_2 injections on changes in coal permeability and swelling effects of adsorbed CO_2 (structure of the coal pore system) the phase 3 of helium flooding experiment was performed. The results are presented in Fig. 7b along with the results of the phase 2 of the He flooding experiments, *i.e.* before and after N_2 injection.

At confining pressures less than 2 MPa, no considerable change in the permeability of the coal sample was observed. However, at higher pressures and constant confining conditions, slight increases and decreases in the coal permeability was observed. Inconsistency between the results at different confining pressures can be attributed to the minor differences in the experimental conditions or slight changes in the coal structure during several cycles of loading and unloading. Overall, no significant improvement in terms of recovery of coal permeability has been observed as a result of N_2 injection.

4.3. CH_4 flooding experiment

Compared to N_2, CH_4 has higher affinity to coal but still lower than that of CO_2 (Hadi Mosleh, 2014). It has been also shown that its volumetric effect on coal matrix is very small, *e.g.* Battistutta et al., 2010. Therefore, CH_4 was injected into the sample to study the potential displacement of the adsorbed CO_2 and further improvement of the coal permeability. Fig. 7c shows the results of the coal permeability variations for two sets of helium flooding experiments conducted before and after the CH_4 injection.

At lower pressures, permeability changes were found to be small. At higher pressures, however, the coal permeability improved which can be partly related to the decrease in the cleat compressibility due to the increase in pore pressures. On average, the permeability of the coal sample was found to increase by 1.6 times as a result of CH_4 injection.

Although, some researchers (De Silva and Ranjith, 2012; Battistutta et al., 2010) have suggested that the swelling effect is a fully reversible process, for the coal sample of this study the swelling effects were found to be only partially reversed during CH_4 injection. This can be attributed to both hysteresis effect and higher affinity of coal to adsorb and retain CO_2 compared with CH_4. Accordingly, the coal permeability was also restored to some extent. Nonetheless, the time dependency of such processes should also be taken into account when interpreting the results (Fokker and van de Meer, 2004). On the other hand, the results of this investigation showed that CO_2 can be adsorbed to the coal to a great extent and changes in gas partial pressure does not lead to a significant and sudden release of adsorbed CO_2. Such data are crucial for assessing long-term stability of the injected CO_2 in coal reservoirs, in applications such as carbon sequestration process in coal seams.

5. Conclusions

The results of this study have provided new insights into the interactions between various gas species in a high rank coal from the South Wales coalfield. Such data-set at this level of accuracy and comprehensiveness is believed to be produced for the first time for the South Wales coals. Using a developed triaxial core flooding setup, a sequence of flooding tests have been designed and conducted to simulate and study two key aspects related to geological sequestration of CO_2 in coal, *i.e.* efficiency of the injection and stability of stored gas due to potential changes in the reservoir pressure. It was shown that the coal permeability has a different level of dependency on the effective stress for different gas species. Especially, the behaviour was highlighted for the case of CO_2 flooding experiments in which the gas adsorption/desorption in coal demonstrated strong effect on the overall permeability evolution. The effect of N_2 on permeability evolution of the coal sample was found to be negligible, whereas the absolute permeability of the coal sample was found to be reduced by 95% as a result of coal matrix swelling induced by CO_2 adsorption at 6 MPa confining pressure. Notably studied in this work, by performing sequential core

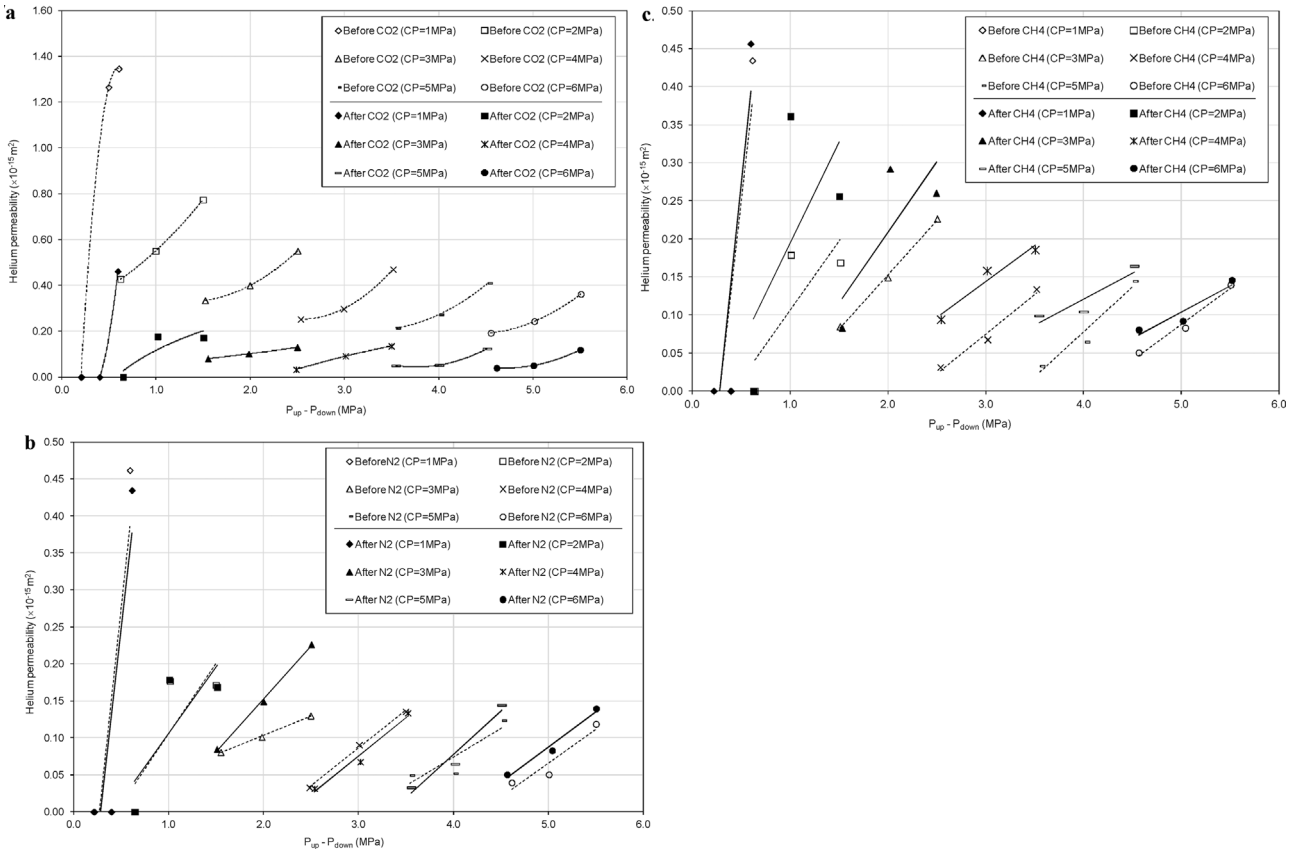

Fig. 7. (a) Variations of the helium permeability of the coal sample with differential gas pressure before (dashed line) and after (solid line) CO_2 injections (T = 298 K). (b) Variations of the helium permeability of the coal sample with differential gas pressure before (dashed line) and after (solid line) the phase 2 of N_2 injections (T = 298 K). (c) Variations of the helium permeability of the coal sample with differential gas pressure before (dashed line) and after (solid line) the CH_4 injections (T = 298 K).

flooding experiments using non-reactive and reactive gases, the chemically-induced strain due to gas sorption into coal has been isolated and quantified from the mechanically-induced strain as a result of changes in effective stress conditions. New dataset generated from the permeability tests are of importance for developing appropriate constitutive relationships/models for permeability evolution in coal that requires reflecting the chemo-mechanical interactions between CO_2 and coal in carbon sequestration and/or enhanced methane recovery.

The results of post CO_2 core flooding experiments using He and N_2 indicated no significant changes in the coal permeability and reversibility of the coal matrix swelling. The injection of CH_4 into the coal sample, on the other hand, resulted in relatively considerable improvement in gas flow rates, so that the initial permeability of the coal sample was restored by an average of 20%. However, the initial permeability of the coal sample was not fully recovered. Based on the results of permeability evolution during post CO_2 flooding tests a relative stability of the stored CO_2 in coal under the experimental conditions/duration was observed.

Acknowledgements

The financial support received from the Welsh-European Funding Organisation as part of the SEREN project is gratefully acknowledged. The authors would like to thank Dr. Snehasis Tripathy for his helpful discussions and support. We wish to thank the GDS Instruments for their contribution for construction and commissioning of laboratory equipment. Technical support from the technicians and staff of the Engineering Workshop at Cardiff University is gratefully acknowledged.

References

ASTM Standards, 1988. In: Donaghe, R.T., Chaney, R.C., Silver, M.L. (Eds.), ASTM STP-977, 1988. Advanced Triaxial Testing of Soil and Rock. ASTM International, West Conshohocken, PA.

Battistutta, E., van Hemert, P., Lutynski, M., Bruining, H., Wolf, K.H., 2010. Swelling and sorption experiments on methane, nitrogen and carbon dioxide on dry Selar Cornish coal. Int. J. Coal Geol. 84 (1), 39–48.

Carman, P.C., 1956. Flow of Gases Through Porous Media. Butterworths, London.

Chen, Z., Huan, G., Ma, Y., 2006. Computational Methods for Multiphase Flows in Porous Media (Computational Science and Engineering). Society for Industrial and Applied Mathematics (SIAM), Philadelphia.

Connell, L.D., Sander, R., Pan, Z., Camilleri, M., Heryanto, D., 2011. History matching of enhanced coal bed methane laboratory core flood tests. Int. J. Coal Geol. 87 (2), 128–138.

Dabbous, M.K., Reznik, A.A., Taber, J.J., Fulton, P.F., 1974. The permeability of coal to gas and water. SPE J. 14 (6), 563–572.

De Silva, P.N.K., Ranjith, P.G., 2012. Advanced core flooding apparatus to estimate permeability and storage dynamics of CO_2 in large coal specimens. Fuel 104, 417–425.

Durucan, S., Edwards, J.S., 1986. The effects of stress and fracturing on permeability of coal. Min. Sci. Technol. 3 (3), 205–221.

Fokker, P.A., van de Meer, L.G.H., 2004. The injectivity of coalbed CO_2 injection wells. Energy 29 (9–10), 1423–1429.

Gan, H., Nandi, S.P., Walker Jr., P.L., 1972. Nature of the porosity in American coals. Fuel 51 (4), 272–277.

Gensterblum, Y., van Hemert, P., Billemont, P., Battistutta, E., Busch, A., Krooss, B.M., De Weireld, G., Wolf, K.H.A.A., 2010. European inter-laboratory comparison of high pressure CO_2 sorption isotherms II: natural coals. Int. J. Coal Geol. 84 (2), 115–124.

Hadi Mosleh, M., Sedighi, M., Vardon, P.J., Turner, M., 2017a. Efficiency of carbon dioxide storage and enhanced methane recovery in a high rank coal. Energy & Fuels 88 (1), 015108. http://dx.doi.org/10.1021/acs.energyfuels.7b02402.

Hadi Mosleh, M., Turner, M., Sedighi, M., Vardon, P.J., 2017b. High pressure gas flow, storage and displacement in fractured rock—experimental setup development and application. Rev. Sci. Instrum. 88 (015108), 1–14.

Hadi Mosleh, M., 2014. An Experimental Investigation of Flow and Reaction Processes During Gas Storage and Displacement in Coal. PhD Thesis. Cardiff University.

Harpalani, S., Chen, G., 1997. Influence of gas production induced volumetric strain on permeability of coal. Geotech. Geol. Eng. 15 (4), 303–325.

Harpalani, S., Mitra, A., 2010. Impact of CO_2 injection on flow behavior of coalbed

methane reservoirs. Transp. Porous Media 82 (1), 141–156.
Hosking, L., 2014. Reactive Transport Modelling of High Pressure Gas Flow in Coal. PhD Thesis. Cardiff University.
Huy, P.Q., Sasaki, K., Sugai, Y., Ichikawa, S., 2010. Carbon dioxide gas permeability of coal core samples and estimation of fracture aperture width. Int. J. Coal Geol. 83 (1), 1–10.
Jasinge, D., Ranjith, P.G., Choi, S.K., 2011. Effects of effective stress changes on permeability of latrobe valley brown coal. Fuel 90 (3), 1292–1300.
Kelemen, S.R., Kwiatek, L.M., Lee, A.G.K., 2006. Swelling and sorption response of selected Argonne premium bituminous coals to CO_2, CH_4, and N_2. In: Proceedings of International CBM Symposium. Tuscaloosa, Alabama.
Laubach, S.E., Marrett, R.A., Olson, J.E., Scott, A.R., 1998. Characteristics and origins of coal cleat: a review. Int. J. Coal Geol. 35, 175–207.
Massarotto, P., Golding, S.D., Iyer, R., Bae, J.S., Rudolph, V., 2007. Adsorption, porosity and permeability effects of CO_2 geosequestration in Permian coals. In: International Coalbed Methane Symposium. Alabama, USA. (CD ROM Paper 0727).
Mazumder, S., Wolf, K., 2008. Differential swelling and permability change of coal in response to CO_2 injection for ECBM. Int. J. Coal Geol. 74 (2), 123–138.
Mazzotti, M., Pini, R., Storti, G., 2009. Enhanced coalbed methane recovery. J. Supercrit. Fluids 47 (3), 619–627.
McKee, C.R., Bumb, A.C., Koenig, R.A., 1988. Stress-dependent permeability and porosity of coal and other geologic formations. SPE Form. Eval. 3 (1), 81–91.
Mehio, N., Dai, S., Jiang, D., 2014. Quantum mechanical basis for kinetic diameters of small gaseous molecules. J. Phys. Chem. A 118 (6), 1150–1154.
Olson, J.E., Laubach, S.E., Lander, R.H., 2009. Natural fracture characterization in tight gas sandstones: integrating mechanics and diagenesis. AAPG Bull. 93 (11), 1535–1549.
Palmer, I., Mansoori, J., 1998. How permeability depends on stress and pore pressure in coal beds—a new model. SPE Reserv. Eval. Eng. 1 (6), 539–544.
Pan, Z., Connell, L.D., Camilleri, M., 2010. Laboratory characterisation of coal reservoir permeability for primary and enhanced coalbed methane recovery. Int. J. Coal Geol. 82 (3–4), 252–261.
Ranjith, P.G., Perera, M.S.A., 2011. A new triaxial apparatus to study the mechanical and fluid flow aspects of carbon dioxide sequestration in geological formations. Fuel 90 (8), 2751–2759.
Salimzadeh, S., Khalili, N., 2015. Three-dimensional numerical model for double-porosity media with two miscible fluids including geomechanical response. Int. J. Geomech. 16 (3).
Sasaki, K., Fujii, K., Yamaguchi, S., Ohga, K., Hattori, K., Kishi, Y., 2004. CO_2 gas permeability and adsorption of coal samples in consideration of CO_2 sequestration into coal seams. J. Min. Mater. Process.Inst. Jpn. 120 (8), 461–468.
Seidle, J.R., Huitt, L.G., 1995. Experimental measurement of coal matrix shrinkage due to gas desorption and implications for cleat permeability increases. In: Proceedings of International Meeting on Petroleum Engineering. 14–17 November, Beijing, China. SPE 30010.
Shi, J.-Q., Durucan, S., 2003. A bidisperse pore diffusion model for methane displacement desorption in coal by CO_2 injection. Fuel 82 (10), 1219–1229.
Siriwardane, H., Haljasmaa, I., McLendon, R., Irdi, G., Soong, Y., Bromhal, G., 2009. Influence of carbon dioxide on coal permeability determined by pressure transient methods. Int. J. Coal Geol. 77 (1–2), 109–118.
Smits, A.J., Dussauge, J.P., 2006. Turbulent Shear Layers in Supersonic Flow, 2nd ed. American Institute of Physics, New York.
Somerton, W.H., Soylemezoglu, I.M., Dudley, R.C., 1975. Effect of stress on permeability of coal. Int. J. Rock Mech. Min. Sci. Geomech. Abstr. 12 (1), 129–145.
Tsotsis, T.T., Patel, H., Najafi, B.F., Racherla, D., Knackstedt, M.A., Sahimi, M., 2004. Overview of laboratory and modelling studies of carbon dioxide sequestration in coalbeds. Ind. Eng. Chem. Res. 43 (12), 2887–2901.
van Bergen, F., Spiers, C., Floor, G., Bots, P., 2009. Strain development in unconfined coals exposed to CO_2, CH_4 and Ar: effect of moisture. Int. J. Coal Geol. 77 (1–2), 43–53.
van Hemert, P., Wolf, K.A.A., Rudolph, E.S.J., 2012. Output gas stream composition from methane saturated coal during injection of nitrogen, carbon dioxide, a nitrogen-carbon dioxide mixture and a hydrogen-carbon dioxide mixture. Int. J. Coal Geol. 89, 108–113.
Vishal, V., Ranjith, P.G., Singh, T.N., 2013. CO_2 permeability of Indian bituminous coals: implications for carbon sequestration. Int. J. Coal Geol. 105, 36–47.
Wang, G.X., Wei, X.R., Wang, K., Massarotto, P., Rudolph, V., 2010. Sorption-induced swelling/shrinkage and permeability of coal under stressed adsorption/desorption conditions. Int. J. Coal Geol. 83 (1), 46–54.
Wang, S., Elsworth, D., Liu, J., 2013. Permeability evolution during progressive deformation of intact coal and implications for instability in underground coal seams. Int. J. Rock Mech. Min. Sci. 58 (1), 34–45.
White, C.M., Smith, D.H., Jones, K.L., Goodman, A.L., Jikich, S.A., LaCount, R.B., DuBose, S.B., Ozdemir, E., Morsi, B.I., Schroeder, K.T., 2005. Sequestration of carbon dioxide in coal with enhanced coalbed methane recovery—a review. Energy Fuel 19 (3), 659–724.
Wu, Y.-S., Pruess, K., Persoff, P., 1998. Gas flow in porous media with Klinkenberg effects. Transp. Porous Media 32, 117–137.
Yu, H., Zhou, L., Guo, W., Cheng, J., Hu, Q., 2008. Predictions of the adsorption equilibrium of methane/carbon dioxide binary gas on coals using Langmuir and ideal adsorbed solution theory under feed gas conditions. Int. J. Coal Geol. 73 (2), 115–129.